IMPLEMENTATION OF A LASER-TRUSS BASED METROLOGY SYSTEM AT THE LARGE BINOCULAR TELESCOPE

by

Stephanie Rodriguez

A Thesis Submitted to the Faculty of the

JAMES C. WYANT COLLEGE OF OPTICAL SCIENCE

In Partial Fulfillment of the Requirements

For the Degree of

MASTER OF SCIENCE

In the Graduate College

THE UNIVERSITY OF ARIZONA

2020

THE UNIVERSITY OF ARIZONA
GRADUATE COLLEGE

As members of the Master's Committee, we certify that we have read the thesis prepared by **Stephanie Lamar Rodriguez**, titled ***Implementation of a Laser-truss Based Telescope Metrology System at the Large Binocular Telescope*** and recommend that it be accepted as fulfilling the thesis requirement for the Master's Degree.

Professor Dae Wook Kim, Chair Date: 08/20/2020

Professor James T. Schwiegerling Date: 8/20/2020

Dr. Hoejoo Choi Date: 08/20/2020

Dr. Andrew Rakich Date: 8/21/2020

Final approval and acceptance of this thesis is contingent upon the candidate's submission of the final copies of the thesis to the Graduate College.

I hereby certify that I have read this thesis prepared under my direction and recommend that it be accepted as fulfilling the Master's requirement.

Professor Dae Wook Kim Date: 08/20/2020
Master's Thesis Committee Chair
Wyant College of Optical Sciences

Acknowledgements

First, I would like to thank Dr. Dae Wook Kim for his endless optimism, kindness, and support as an advisor. Next, I would like to thank Dr. Heejoo Choi for all his help and guidance. His selfless dedication to the group is truly unparalleled. Also, thank you for making all those long trips up the mountain with me and driving halfway. I would also like to thank Dr. Andrew Rakich for sharing his wide breadth of knowledge with enthusiasm and patience. I learned something new every time we spoke. Thank you to Dr. Christian Veillet, Dr. John Hill, and Dr Olga Kuhn at LBTO for their invaluable insight. I would also like to give my thanks to the mountain crew at LBT who always offered their help while working on site. I am profoundly grateful for the opportunity to work on such an incredible system with such an incredible group of people.

Thank you to all my LOFT peers. Their friendship was vital to my success and I am constantly inspired by all that they accomplish. I would like to thank WiO for their dedication to marginalized members of the optics community and for making OSC a more welcoming and inclusive place. Also, thank you to all the friends I made at OSC.

I would like to thank all my friends and family for their unwavering faith in me. I would not be the person I am today without your love and support. A special thanks to my brother for being my best friend since day one.

Thank you, Riley, for everything.

Dedication

For Tim Butcher.

Never stop searching for the light.

Table of Contents

List of Figures

List of Tables

ABSTRACT

Large ground-based telescopes are prone to perturbations caused by environmental factors that affect the mechanical structure of the telescope that can cause collimation loss and image quality degradation. The Telescope Metrology System (TMS) is a metrology method under development at the Giant Magellan Telescope (GMT) and prototyped on the Large Binocular Telescope (LBT) to monitor and maintain collimation and pointing. TMS measures the precise position and orientation of a telescope's primary mirror in relation to other telescope elements. Currently, prototyping has progressed to TMS operation at prime focus between LBT's two 8.4m primary mirrors and the Large Binocular Camera (LBC), a pair of prime focus correctors and wide-field detectors. TMS utilizes a multi-channel absolute distance measuring (ADM) interferometer to create a laser truss by determining the distance between fixed points on the primary mirror and the LBC. By performing a kinematic analysis of the ADM data, the relative position and orientation of the primary mirror and the LBC can be determined. With knowledge of the position of the telescope a model can be created using TMS data as input. This allows for iterative simulation of field aberrations and loss in image quality due to misalignment of the telescope. This will allow for collimation and pointing to be actively monitored and maintained during an observation. This paper will discuss the process of implementing TMS on LBT and the challenges that arose.

1. INTRODUCTION

1.1 Large Binocular Telescope

The Large Binocular Telescope (LBT) is located atop Mount Graham in southeastern Arizona sitting at an elevation of 3200m. It is comprised of two Gregorian telescopes on a common altitude and azimuth mount (Figure 1). Each telescope has an 8.4m primary mirror. This gives the telescope an 11.8 m effective aperture and a 22.8 m interferometric baseline. LBT is host to a suite of scientific instruments including optical wide field cameras (LBC), several spectroscopic instruments (LUCI, MODS, and PEPSI), and interferometric instruments (e.g. LBTI). To accommodate the various science instruments the telescope operates at prime focus as well as at bent and direct Gregorian modes as shown in Figure 2. To engage Gregorian and bent Gregorian modes there are deployable adaptive secondary mirrors and tertiary mirrors [1]. Operating such a large and complex optical system at seeing limited resolution requires a sophisticated active optics system to compensate for environmental perturbations.

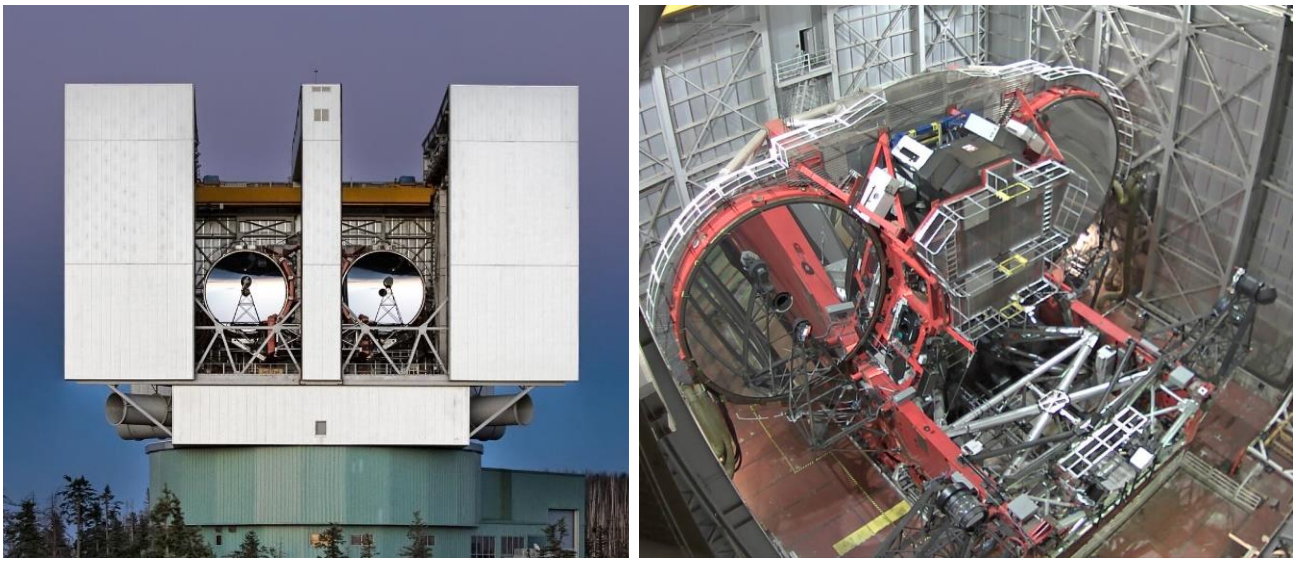

Figure 1 Large Binocular Telescope with the dome open atop Mount Graham at dusk during the beginning of observation. The two 8.4m primary mirrors are on a common altitude and azimuth mount. The entire 25m tall dome structure, weighing 700 tons rotates, on the azimuth at speeds up to 1° per second [2].

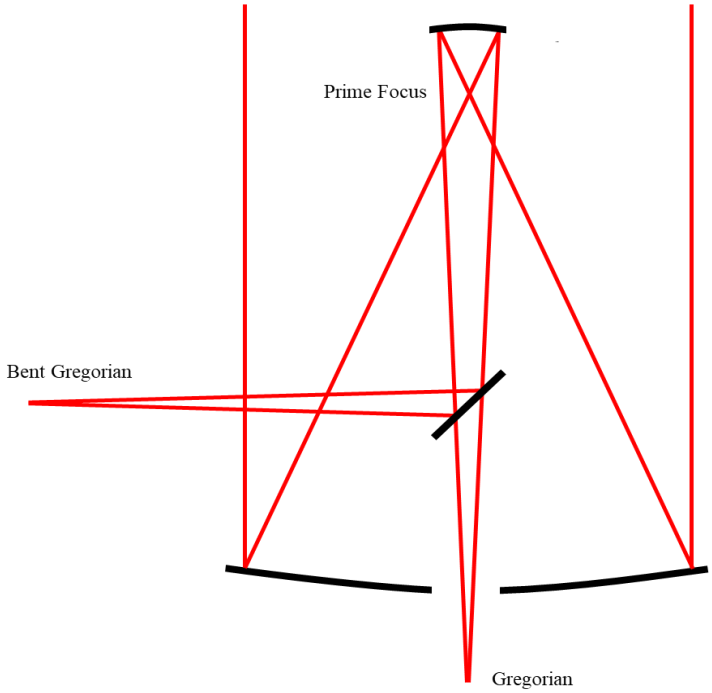

Figure 2 Focal stations on LBT. Each mirror has three focus modes: prime focus, Gregorian, and bent Gregorian. Prime focus has a single focal station operating at F/1.142. The Gregorian and bent Gregorian modes operate at F/15 [2]. Prime focus is engaged for use with the Large Binocular Camera (LBC).

The Large Binocular Cameras are the prime focus instruments on LBT(Figure 3). Each side of the binocular houses one camera on a deployable arm. The cameras can be operated together in binocular mode, or individually in monocular mode. LBC red operates from 550nm to 1 micron. LBC blue operates from 350nm to 650nm. The combination of the two cover the optical spectral range and allow simultaneous deep imaging in two filters. They both offer wide fields of view of 23 arcmin x 25 arcmin. The detector is covered by four 2048x4806 pixel CCDs. Three are aligned side by side and a fourth lies above the other three and is rotated 90 degrees. The pixels are 13.5x13.5 microns and cover 0.226 arcseconds on the sky [3].

Table 1 Large Binocular Camera Specifications

Specification	Value
Spectrum	LBC blue 350nm-650nm LBC red 550nm-1000nm
Field of view	23arcmin x 25arcmin
Detector	4 CCD array
Pixel per detector	2048x4806 pixel
Pixel scale	13.5x13.5 micron
Angular resolution	0.226 arcsec/pixel

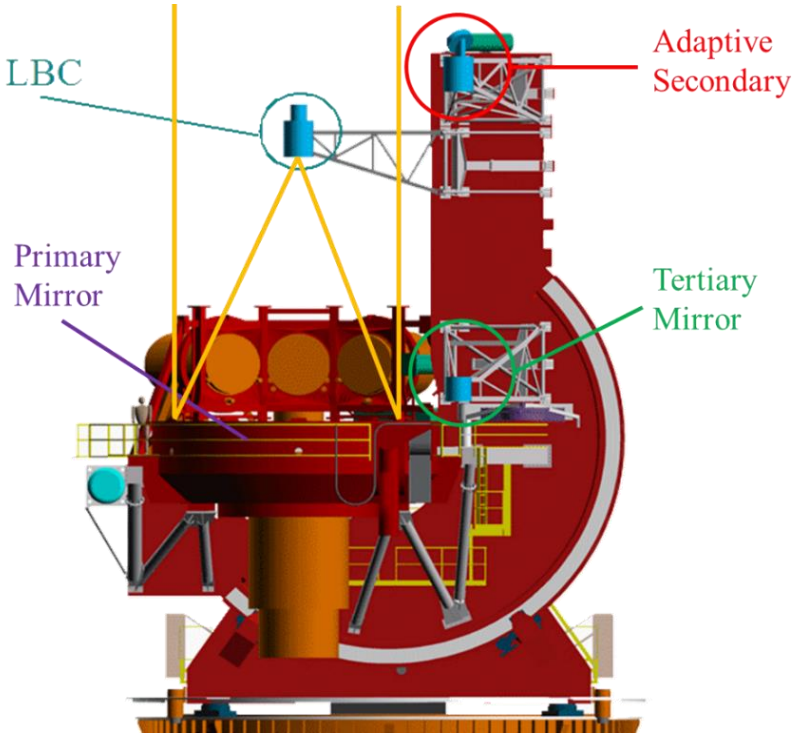

Figure 3 LBT with prime focus engaged for use with the Large Binocular Camera (LBC) deployed. The adaptive secondary mirror and the tertiary mirror are housed on deployable swing arms and can be moved into the optical axis to engage Gregorian and bent Gregorian focal modes.

1.2 Collimation and pointing

When operating a telescope, it is crucial to maintain collimation and pointing over an exposure. Failure to do so can cause image quality degradation via aberration or image trailing. Telescope collimation refers to the alignment of the system's optical elements. A telescope is collimated when all optical elements are aligned properly, centered about their optical axis, and focus the light onto the image plane. A well collimated telescope will provide good image quality free from aberrations due to misalignment, although aberrations from other sources may be present. Pointing is the process of slewing the telescope to objects in the sky and following the objects during observation. LBT is on a mechanical azimuth and altitude mount which controls gross pointing as shown in Figure 4.

Large telescopes are especially prone to misalignments caused by the mechanical changes needed to maintain pointing. Changes in altitude and azimuth cause changes in the gravitational effects felt by the optics, especially the primary mirror (Figure 5). Controlled motion of the primary mirror is the main collimation control. This requires adjustment of the primary mirror to maintain collimation. In turn this adjustment can cause the telescope to lose pointing. LBC does not require absolute pointing at the beginning of an exposure. Therefore, these pointing changes do not strongly constrain collimation. Once the exposure begins pointing must be maintained [4]. Exposures can last from seconds to hours. A balance must be met to ensure that image quality does not degrade during observation. Maintaining collimation and pointing is especially important when using a wide field instrument such as the LBC.

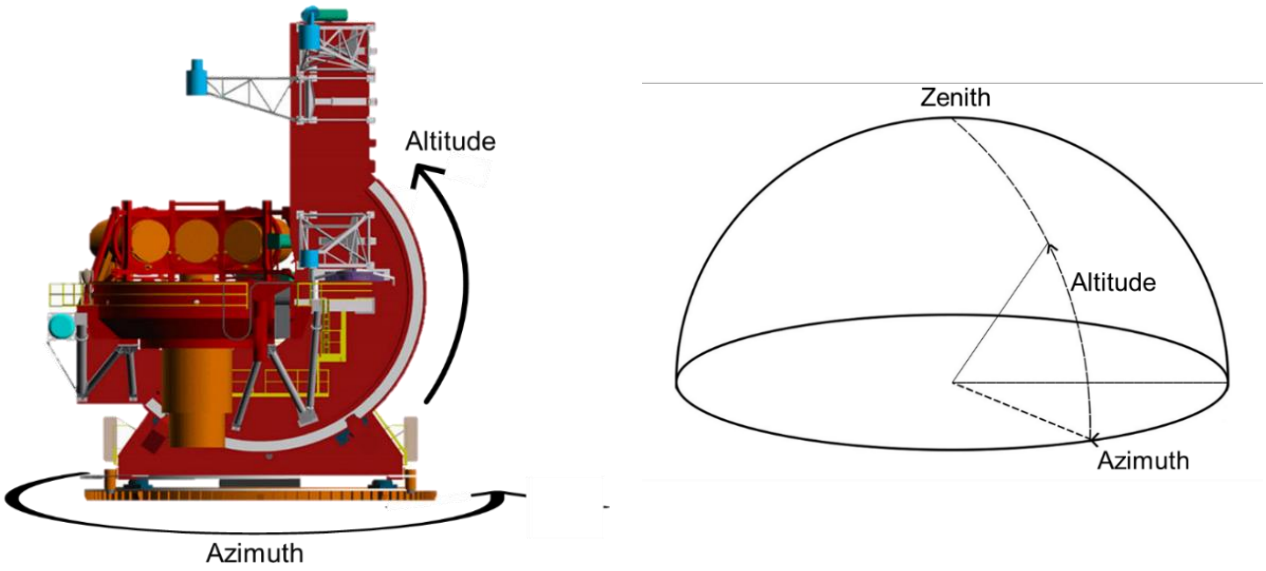

Figure 4 Telescope pointing control. LBT is on a common altitude and azimuth mount. The telescope (left) is pictured at zenith. Azimuth is controlled by rotation of the entire structure. Altitude changes occur along the c-ring structure [2].

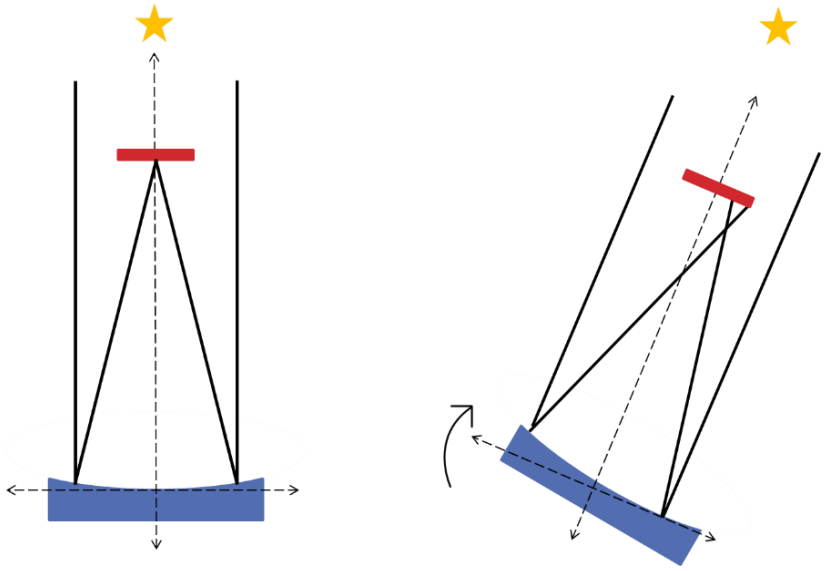

Figure 5 A well collimated telescope (left) will focus light onto the image plane. As the telescopes positions changes to track an object over the sky (right) the optics that were once well collimated can be deflected by mechanical changes in the telescope. This causes loss of collimation and aberration in the image.

1.3 Active optics on the Large Binocular Telescope

Large ground-based telescopes are affected by various environmental factors including: mechanical deflections due to gravitational forces, thermal effects, and hysteresis. Active optics are used to mitigate these environmental factors and are an essential part of any ground-based telescope. Active optics corrects larger low order aberrations on longer time scales. This allows the dynamic range of

the adaptive optics system to be conserved for smaller aberrations that occur over very short time scales. LBT has a multifaceted active optics system. Active optics can be used to correct lower order aberrations such as tip, tilt, coma, and astigmatism.

The telescope is outfitted with Acquisition, Guiding, and Wavefront (AGW) sensing unit as part of the active optics system. Unfortunately, the LBC is unable to utilize the AGW due to design flaws and therefore it will not be covered in the scope of this paper. LBC uses extra-focal pupil imaging to measure the wavefront, along with control loops to drive the prime focus active optics. The extra-focal images are produced by movement of the primary mirror along the optical axis as shown in Figure 6. These images are used to collimate the telescope and determine how best to correct aberrations [5]. This allows for measurement of low order aberrations without the need for additional optical elements or wavefront sensors. This process is repeated each time the telescope slews to a new field.

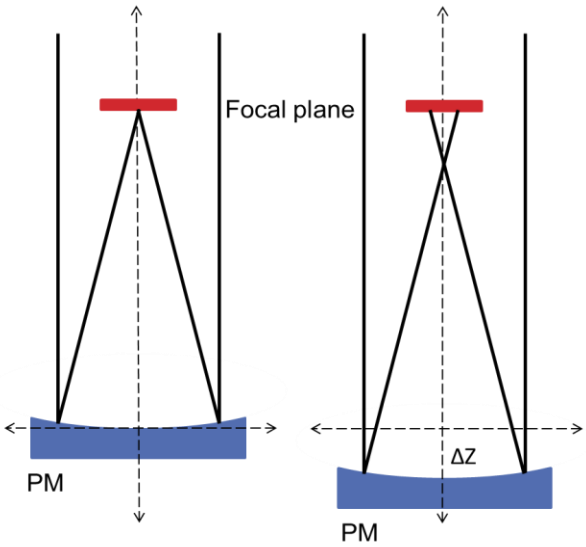

Figure 6 Extra focal imaging acquired through movement of the primary mirror. The extra focal image shape can be used to determine first order aberrations tip, tilt, defocus, coma, and astigmatism.

The primary control algorithm for collimation of LBC is the Focal Plane Image Analysis (FPIA). The FPIA uses a geometric approach to analyze low order aberrations. The extra-focal pupil images are used to determine what corrections need to be made in the alignment of the primary mirror to collimate the telescope. When the telescope is perfectly collimated the extra-focal image is non-aberrated and looks like then entrance pupil of the telescope. The size, centration of the central obscuration, ellipticity, and ratio of central obscuration size to outer diameter of the extra-focal image can determine focus, coma, astigmatism, and spherical aberration respectively [2]. The traditional technique for using defocused pupil images usually involves intra-focal as well as extra-focal pupil images as shown in Figure 7. FPIA uses extra-focal pupil images only but performs the same analysis [5]. Once the aberrations are known the proper corrections to the primary mirror position and shape can be made to improve collimation.

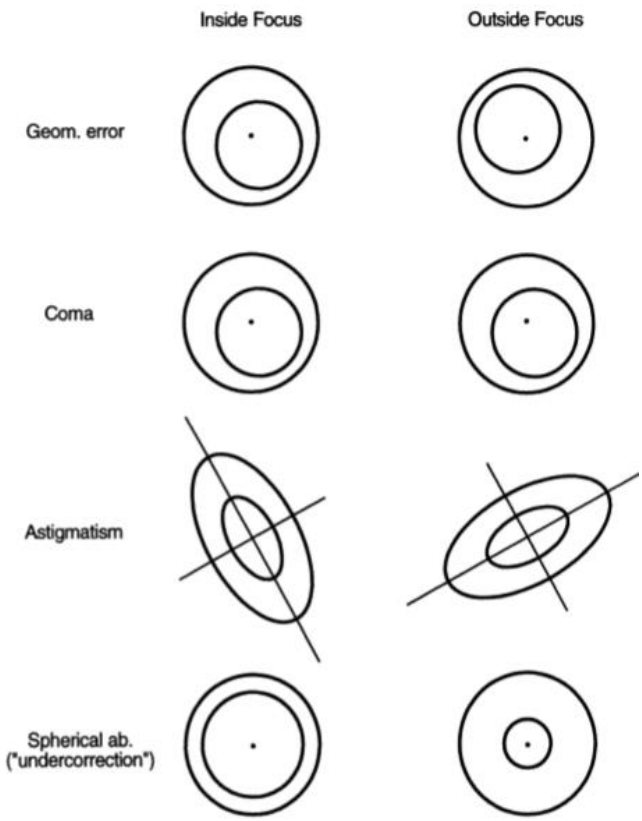

Figure 7 Extra-focal pupil imaging is used to determine calculate first order aberrations present in the system. By measuring the size of the central obscuration, the diameter of the pupil image, and the ellipticity defocus, coma, astigmatism, and spherical aberration can be determined. This information can be used to actively control and correct the collimation of the telescope [6].

The extra-focal pupil technique is useful for achieving collimation at the beginning of acquiring a new field. However, as mentioned in Section 1.2 collimation and pointing must be maintained over the duration of an exposure. Once an exposure has begun the telescope cannot be defocused to obtain the extra-focal pupil images for analysis. Since FPIA is the main active control method for observation with LBC, LBT is left in a vulnerable position during an exposure. Currently a series of look up tables are used to position the primary mirror to maintain collimation while at various elevations and under given environmental conditions. These look up tables provide gross correction, but struggle to achieve and maintain good image quality in adverse thermal conditions. The look up tables could be updated and refined with the help of the metrology system described in this paper, although the ultimate goal is to use the system for active control. If collimation is lost during an exposure can cause of loss of seeing-limited telescope performance. Therefore, another technique must be developed to help ensure that collimation can be monitored and maintained over an exposure while still achieving proper pointing.

1.4 Telescope Metrology System background and configuration

The Telescope Metrology System (TMS) measures the precise position and orientation of a telescope's primary mirror in relation to other optical elements. This allows for collimation and pointing to be monitored and maintained during observation without the need for wavefront sensing or image analysis. This is a particular interest in regard to use of prime focus on LBT since, as discussed in Section 1.3, other active elements are not available for use with LBC while an exposure is underway.

The Telescope Metrology System is an ongoing development program created by staff at the Giant Magellan Telescope (Figure 8) [7]. Since 2017 there has been a mutually beneficial collaboration between LBT and GMT. TMS was installed on LBT to act as a testbed for the planned GMT metrology method. LBT's two 8.4m primary mirrors are approximately the same size each of the seven segmented mirrors on GMT [8]. This allows GMT to develop and characterize the system, while also adding an element to LBT's active optics system. The prototyping of TMS on LBT is a three phase process. The first phase, acquiring a working TMS for use at prime focus, is covered in the scope of this paper. The next two phase are outside the scope of this paper involve the use of TMS at bent Gregorian and in interferometric observation.

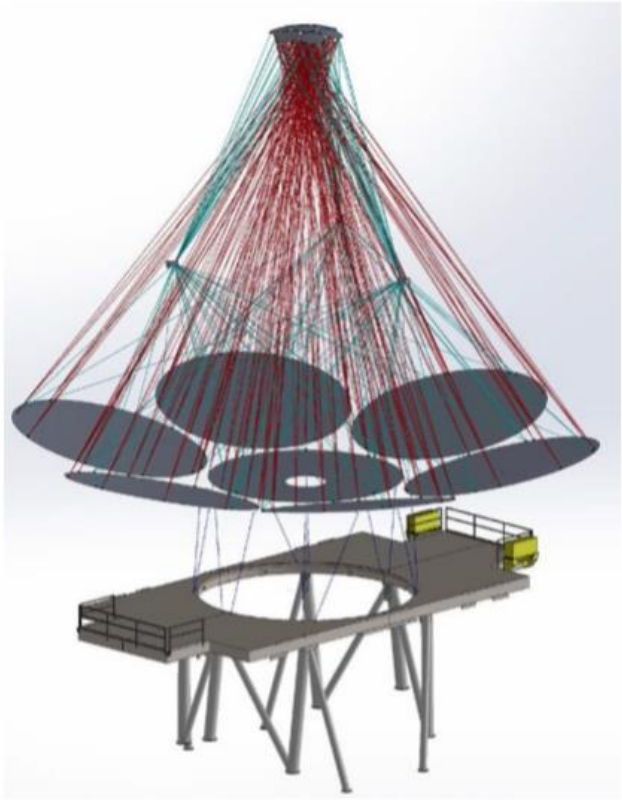

Figure 8 Giant Magellan Telescope laser truss metrology system. The Telescope Metrology System was developed as a component of the active optics system to be implemented on GMT. GMT has seven telescope units with 8.4m primary mirror segments conjugate to a seven segmented secondary mirror. Each primary mirror will have 9 laser truss legs, totaling 81 laser truss measurement channels [8].

1.5 Overview and system requirements

The Telescope Metrology System uses changes in distance from points around the primary mirror to retroreflectors on the prime focus instrument to calculate the precise position and orientation, or "pose," of the two elements in relation to one another. Using a multichannel absolute distance measure interferometer, a laser truss is created between collimators positioned around the primary mirror and retroreflectors on LBC. If LBC is taken to be fixed the changes in lengths of the legs of the laser truss can be used to determine the relative movement of the primary mirror in 6 degrees of freedom: lateral x, y, and z movement and rotational Rx, Ry, and Rz movement. Knowledge of the precise position of the primary mirror can be a valuable tool in an active optics control system.

TMS operates without the need for wavefront sensing elements and without adding any additional optical elements in the telescope's optical path [8]. The measurement channel hardware is comprised of fiber routed to the telescope, collimators around the primary mirror, and retroreflectors mounted on LBC and other parts of the mechanical structure of the telescope. All hardware elements are attached to mechanical structures, to passively monitor the position of the optical elements. Collimators are mounted around the primary mirror cell as shown in Figure 9 and Figure 10. The collimators are aligned to fiducials on LBC to create the laser truss.

Figure 9 Collimators are mounted around the primary mirror cell. Fibers are routed from the Etalon in the auxiliary room off of the dome, onto the telescope and to the collimators. The mounts are comprised of off the shelf components, making them modular and easy to reconfigure. A ball mount allows for large adjustments in collimator pointing. The collimators are housed in precision kinematic mounts for fine alignment adjustment.

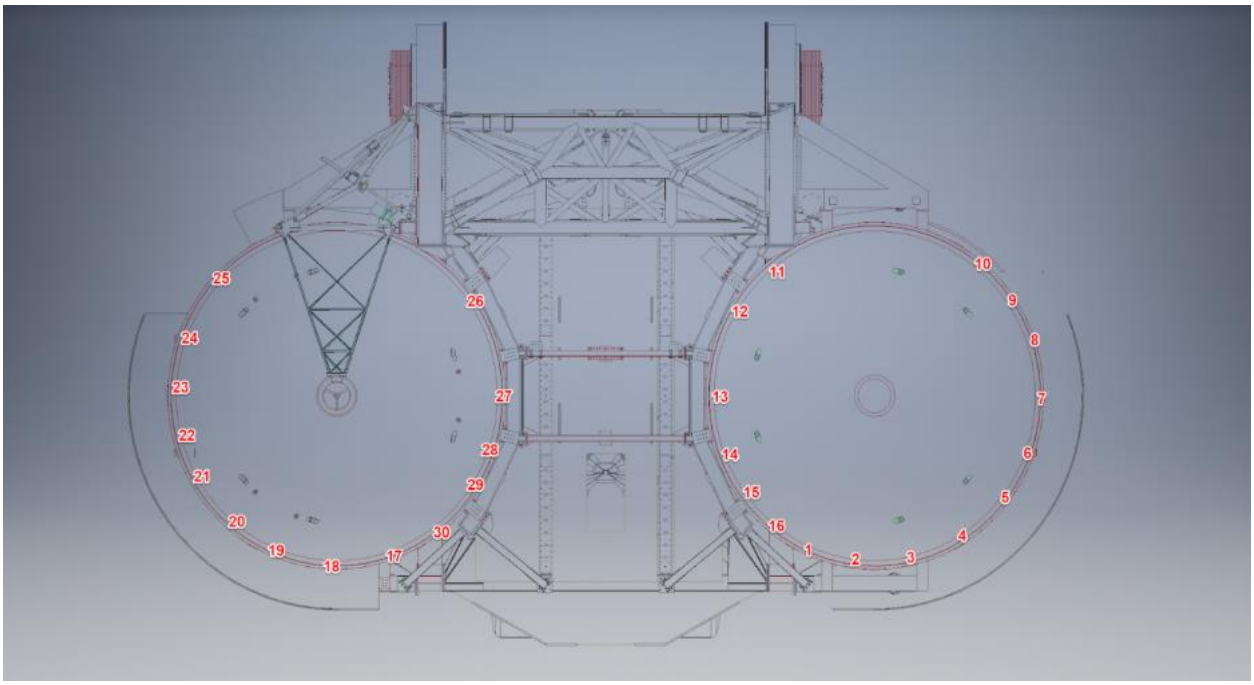

Figure 10 Primary mirror cell positions around DX and SX. There are a total of 30 mirror cell mounts attached directly to the primary mirror cells using silicone sealant and Invar base, so as to prevent damage to the primary mirror do to thermal expansion. The collimator mounts are then magnetically coupled to the mirror cell cases.

The legs of the laser truss are measurement arms of the TMS interferometry system. To measure the distance between the collimators and retroreflectors TMS utilizes an Etalon Absolute Multiline Technology (EAMT). The EAMT is an absolute distance measuring interferometer that uses a dynamic frequency scanning technique capable of measuring multiple channels with micron level accuracy. The ability to simultaneously measure many channels is especially useful for TMS, as the kinematic analysis requires a minimum of 6 channels to calculate the relative position and orientation of the primary mirror. This also allows for redundant laser truss channels and additional channels needed to measure the diameter of the primary mirror and for use at Gregorian and bent Gregorian focus in the next phases of the project.

A kinematic analysis is performed to translate laser truss leg measurements from the EAM into position and orientation information, or “pose” of the LBC correctors to the primary mirror. The kinematic analysis is based on the mechanical principle of a Stewart-Gough hexapod platform, in which the desired motion of a platform relative to its base is induced by controlled changes in the legs of the platform. The TMS requires known changes in leg length to determine the motion of the system elements. This is done through an inverse kinematic technique described later in Section 3.2 Hexapod inverse kinematics using Matlab. The kinematic analysis gives the relative position and orientation of the primary mirror.

The primary mirrors has 6 degrees of freedom of motion lateral xyz motion and rotational Rx Ry Rz. Primary mirror motion is induced by movement of the hexapod hardpoints. Each hardpoint is housed in a cylinder with a diameter of 6mm and a height of 6mm. It is the range of motion of the hardpoints that define the range of motion of the primary mirror. Lateral motion in the x and y direction has a

range of ±2.0 mm while the z direction (along the mirror axis direction) has a range of ±2.6 mm. Rotational motion in Rx, Ry, and Rz has a range of ±100 arcsec. The range of primary mirror motion is summarized in **Error! Reference source not found.**. The primary mirror also has an array of a ctuators that can induce 56 Zernike polynomial terms onto the surface of the mirror that can be used in conjunction with hardpoint motion. The actuators can be used to compensate for mirror bending due to thermal and gravitational effects, as well as alignment aberrations. LBC is deployed on a swing arm at prime focus, and although it can change position due to mechanical deflections of the swing arm, it is considered a fixed element.

Table 2 Primary mirror range of motion

Primary mirror motion	Range
Lateral x and y motion	±2.0 mm
Piston z motion	±2.6 mm
Tip Tilt Rx Ry motion	±100 arc sec
Clocking Rz motion	±100 arc sec
Incremental accuracy	1 micron

1.6 Etalon Absolute Distance Measuring Interferometry System

The Etalon Absolute Multiline Technology (EAMT) is an absolute distance measuring interferometer (Figure 11). The EAMT uses a technique called dynamic frequency scanning to determine distance without ambiguities, even over meters of measurement [9]. The unit on LBT has 28 channels, but the machine can be modified to host up to 124 measurement channels. When airpaths are adequately temperature-sensed and corrected for variation in refractive index of air [10], the EAMT has a measurement uncertainty of 0.5 microns per meter and can measure distances up to 20m. TMS channels on LBT generally range from 8-10m. The expected uncertainty in distance measurement should not significantly impact system performance.

In order to perform the kinematic analysis needed to determine the position and orientation of the primary mirror a minimum of 6 channels are needed, two per fiducial on LBC. To ensure that a calculation can be made even when a channel is lost an extra channel is added to each fiducial on LBC for a total of 9 channels. In addition, 2 channels are used to monitor the diameter of the primary mirror. Each side of the telescope requires a minimum of 11 channels to operate. A total of 22 channels are needed for TMS to operate at prime focus in binocular mode. For the next phases of the project additional channels will be needed.

Figure 11 Etalon Absolute Multiline absolute distance measuring interferometry system. The EAM employs a dynamic frequency scanning interferometry technique using fiber tip Fizeau interferometric patterns to accurately measure distance greater than 20m with an uncertaintiy of 0.5µm/m. The EAM unit itself is stored in an auxiliary room off the telescope dome.

Table 3 Etalon Absolute Multiline specifications

Measurement Channels	Up to 124
Measurement uncertainty	0.5 microns/meter
Measurement Range	<20m
Measurement frequency	500kHz
Channel hardware	Collimator, retroreflector, and telecom fiber
Wavelength band	1530 +/- 70 nm
Calibration	Gas absorption cell
Compensation	Temperature, pressure, and humidity

The Etalon Absolute Multiline is an absolute distance measuring (ADM) interferometer that uses a dynamic frequency scanning interferometry (FSI) technique [9]. FSI utilizes a frequency scanning laser to determine the ratio OPD of two of more interferometers. One interferometer acts as the reference and must have stable known OPD. In a basic FSI system the intensities of the return signal from a single frequency scanning laser as it sweeps over its frequency range are collected. The relative phase over a scanning time interval can then be extracted for each interferometer.

$$\frac{\varphi_i^M}{\varphi_i^R} = \frac{L_M}{L_R}$$

The ratio of the phase of the measurement interferometer φ^M and reference interferometer φ^R are directly proportional to the lengths of their arms for each i^{th} sampled time. This method is limited in that the reference interferometer OPD must be known before the start of the scan and the measurement arm OPD must constant over the duration of the scan.

The dynamic FSI technique uses a second frequency scanning laser and a gas absorption cell to overcome the limitations of a standard FSI system. Introducing a second frequency scanning laser that covers the same range of frequencies but scans in the opposite direction as the first laser creates another interference pattern for each interferometer which have their own set of phase equations φ_{ti}^M. This addition allows for the length to be determined at each sampling time t_i and removes the constraint of a constant measurement arm length over then entire scan. The gas absorption cell creates a spectra of each laser that can be used to define a reference length L_R. With a known L_R the v_{ti} can be determined at any time in the scan. Using the known frequency absorption properties of the gas cell additional equations for the phase φ_{ai}^M at these known frequencies v_{ai} of each laser during a scan. This creates a very stable reference that does not need to be known before the start of a scan. The length of the measurement arm a time t_0 is given by

$$L_{t0} = \frac{v_{t2}\Delta\varphi_{t,a}^{M1} - v_{t1}\Delta\varphi_{t,a}^{M2}}{\frac{4\pi}{c}(v_{a1}v_{t2} - v_{a2}v_{t1})}$$

where $\Delta\varphi_{t,a}^{M1,2}$ is the difference between the measured phase from the interference pattern of each laser and the phase at known frequencies from the gas absorption cell. This creates a very stable reference that does not need to be known before the start of a scan [9].

The Etalon Absolute Multiline uses fiber tip Fizeau interferometry. This allows the measurement channels to be fairly simple. The channels consist of a telecom fiber coupled to a collimator that launches the beam to a retroreflector as shown in Figure 12. The back reflection from the fiber tip is the reference arm of the interferometer and the measurement arm is the path through the collimator to the retroreflector and back. The OPD measured corresponds to the distance between the fiber tip and the retroreflector. Telecom fibers can be run for kilometers if necessary and are easily routed onto the telescope. The Etalon is stored in an auxiliary room off the main dome of the telescope and the fibers are ran out to the telescope. There are also no electronics required on the telescope. This allows the TMS hardware footprint on LBT to remain small.

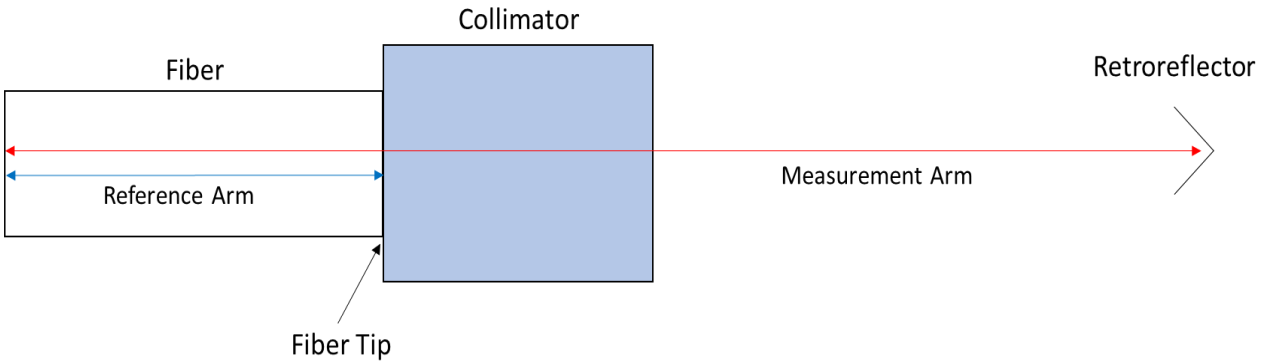

Figure 12 Fiber tip Fizeau interferometry uses back reflections from the tip of the fiber interfered with light that exits the fiber and returns back through the fiber. The TMS system uses a collimator to shoot light from the fiber onto a retroreflector that sends the beam back along this same path.

2. TMS HARDWARE MAINTAINCE AND SYSTEM FUNCTIONALITY

2.1 TMS Status at Beginning of Fall 2019

TMS prototyping on LBT began in 2017. By 2018 TMS was operational for use at prime focus [8]. All needed hardware was installed including: Etalon Absolute Multiline Technology, fibers routed to primary mirror, mirror cell mounts, collimators, retroreflectors on LBC and on mechanical structure of the telescope. A series of testing was performed to characterize the system and validate its functionality.

The first test used to determine the validity of the measurement data was correlating the changes diameter of the primary mirror due as reported by the EAMT to the expected thermal expansion. The primary mirrors are made of borosilicate. Using known thermal expansion of borosilicate and temperature telemetry data from LBT the expected change in mirror diameter can be determined. The Etalon measured an increase of primary mirror diameter due to thermal expansion of approximately 8.4 microns/K, which corresponds closely to the expected value [8].

Passive closed dome and on sky data was also collected and analyze. The closed dome testing was able to demonstrate accurate measuring of the position of the primary mirror using known incremental movements and the EAMT deformation analysis. The tests also revealed that TMS was operable over the full range of motion of the primary mirror. Passive on sky results confirmed that the system was able to operate in open dome conditions, under various weather conditions, with no significant change in system performance. Active on sky performance was also examined. TMS was ran both as the primary source of active control and as an additional element of existing active optics controls. When ran without other active optics controls TMS was able to maintain good image quality over serval hours of LBC observation. When used in addition to other active optics controls, it improved overall active correction performance [8]. By the end of 2018, the validity of TMS operation at prime focus had be tested and verified.

Every summer both primary mirrors are cleaned and recoated. TMS must be removed during this process as it is directly attached to the mirror cell. After the summer 2019 mirror reinstallation, TMS

was also reinstalled. Unfortunately, the system was no longer operational due to improper re-installation. In the fall of 2019, the effort to restore and improve TMS functionality began.

2.2 Regaining TMS functionality

In order to regain TMS functionality the system hardware was assessed and properly reinstalled. This process includes measurement channel signal assessment, collimator selection, laser stability testing, fiber routing, securing mechanical collimator hardware, and collimator alignment. When the collimators are in place and aligned a laser tracker survey is performed to obtain a global reference frame for use in the kinematic analysis. Once these steps are complete TMS data can be captured and used in determining position and orientation using a kinematic analysis technique.

There are three different collimators available: collimator 1 provided by the Etalon company, collimator 2 obtained from Thorlabs, and collimator 3 designed by Andrew Rakich. Lateral tolerancing tests were performed to determine which collimator provides optimal performance when decentered. Each collimator and retroreflector were aligned as shown in Figure 13 at a distance of 5m. The retroreflector was laterally decentered on a translational stage. The signal strength is measured by percent of power returned to the EAMT. Loss of signal power can be caused by decenter or due to beam divergence caused by the collimator. The results of the lateral tolerancing test are shown in Figure 14. The collimator 1 had the worst performance in both signal strength and lateral decenter tolerance of approximately ±1.5mm. The primary mirror has a lateral range of motion of ±2.0mm, therefore collimator 1 would not provide adequate performance over the full range of motion of the primary mirror, resulting in channel loss. Collimator 3 provides the best performance in both signal strength and lateral decenter tolerance of approximately ±2.75mm. Collimator 3 will not cause channel loss due to decentering over the full range of motion of the primary mirror. This was verified practically while performing alignment. Both collimator 1 and collimator 2 are not well collimated over the distances required for TMS. The large beam divergence makes them difficult to align over large distances inside of the telescope dome. It was found that the large black collimators were the easiest to align.

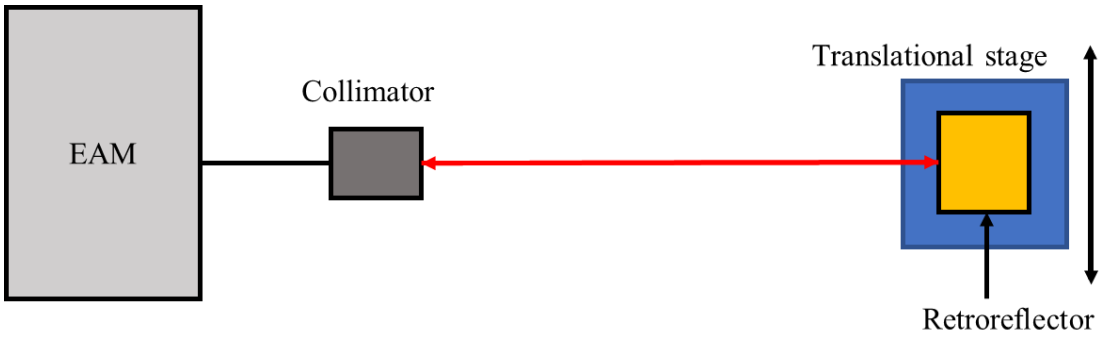

Figure 13 Lateral tolerancing test set up. Each collimator was mounted to a stationary mount and connected to the EAMT. A retroreflector was placed on a translational stage at a distance of 5 m from the collimator. Decenter of the retroreflector was induced and the signal strength as reported by the EAMT was recorded.

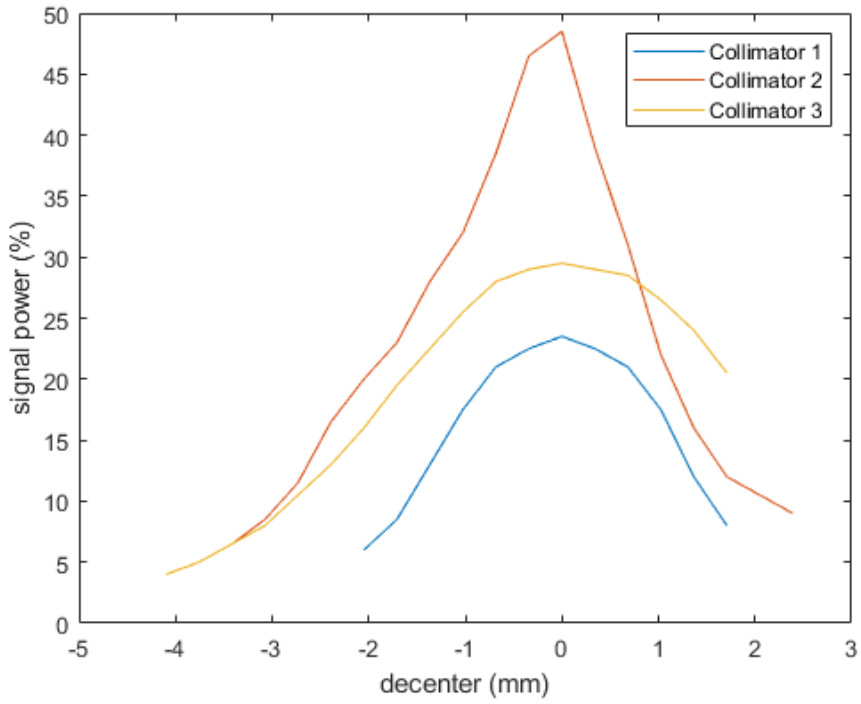

Figure 14 Lateral tolerancing test performed using the three available collimators shows that collimator 3 provides the best performance with a max signal power of 48% and decenter tolerance of ±2.75mm. It is important to have a sufficient decenter tolerance to maintain channel signal over the range of motion of the primary mirror.

The first step to regaining functionality was determining which measurement channels where receiving enough optical signal from the EAMT to make a valid distance measurement. The EAMT configuration on LBT has 28 channels. The first 16 channels have individual fibers that are routed directly to the mirror cells. Channels 17-28 are combined into a multicore fiber that is routed to a MPO cassette located on the telescope. From the MPO cassette channels are routed to mirror cells. There are thirty mirror cell positions around both primary mirrors. The mirror cells positions can house up to two collimators.

A simple quick test was devised to establish the strength and viability of the measurement channels. The test consisted of a collimator and retroreflector were mounted closely together on a common stationary mount shown in Figure 15. This method was found to be more reliable than simply attaching a power meter to the end of the fiber since the EAMT reports percent of signal returned, not a power value. The signal strength of each channel was probed at every connection point along the fiber: at the EAMT, at the MPO, and on the mirror cell. This process helps determine where the signal is lost along the fiber route. This information will also be used to determine what hardware is damaged and what repairs need to be made. The return signal strength from the EAMT software was used to establish the status of the channel. Noise on the channel can give return strength up to 4-5%, which will still produce distance data causing noise error in the TMS kinematic analysis calculations. Therefore, a signal strength of greater than 10% is preferred to produce an accurate measurement and to minimize noise error.

Figure 15 Channel strength test configuration. A collimator and retroreflector are on a common mount. The collimator is aligned to receive maximum return signal from the retroreflector.

The results of the test are summarized in Figure 16. The MPO cassette is noticeably damaged, with all but two channels receiving no signal. The MPO cassette must be replaced at a later date if TMS is to be set up on for use in binocular or interferometric mode. A minimum of 11 channels are needed for TMS operation at prime focus. There are currently fifteen available channels on the mirror cell with enough return signal to make a measurement. Fortunately, that is a sufficient number of channels to deploy TMS in monocular configuration. Nine of these channels are utilized on LBC fiducials, two on primary mirror diameter measurements, and three are used to measure distance from the primary mirror to fixed fiducials on the mechanical structure of the telescope.

With knowledge of operational channels, a configuration of the laser truss is built. Collimators around the primary mirror cell are aligned to retroreflectors on the LBC as shown in Figure 17. Three collimators are aligned to each of the three LBC retroreflectors. This provides a “redundant truss” as in principle six channels to three retroreflectors is the minimum requirement. This redundancy is deemed useful for system stability and error checking. The optimal separation of collimators around the mirror cell per fiducial is 120 degrees. An attempt was made to approach this optimal positioning as the mirror cell position and available channels allowed. Two channels measure the diameter of the primary mirror separated by approximately 90 degrees. Although this is not used in the pose calculations it can be used to monitor and compensate for the thermal expansion of the primary mirror. The schematic of the collimators and retroreflectors is shown in Figure 18. An additional three fiducials are mounted on the mechanical structure of the telescope near the opening towards the bent Gregorian focus and LBTI. Three channels, one per fiducial are aligned to the LBTI fiducials. These channels will be used in phase two and three of TMS prototyping for operation at bent Gregorian and in interferometric mode. Both phases are out of the scope of this paper, but the channels were aligned for future use.

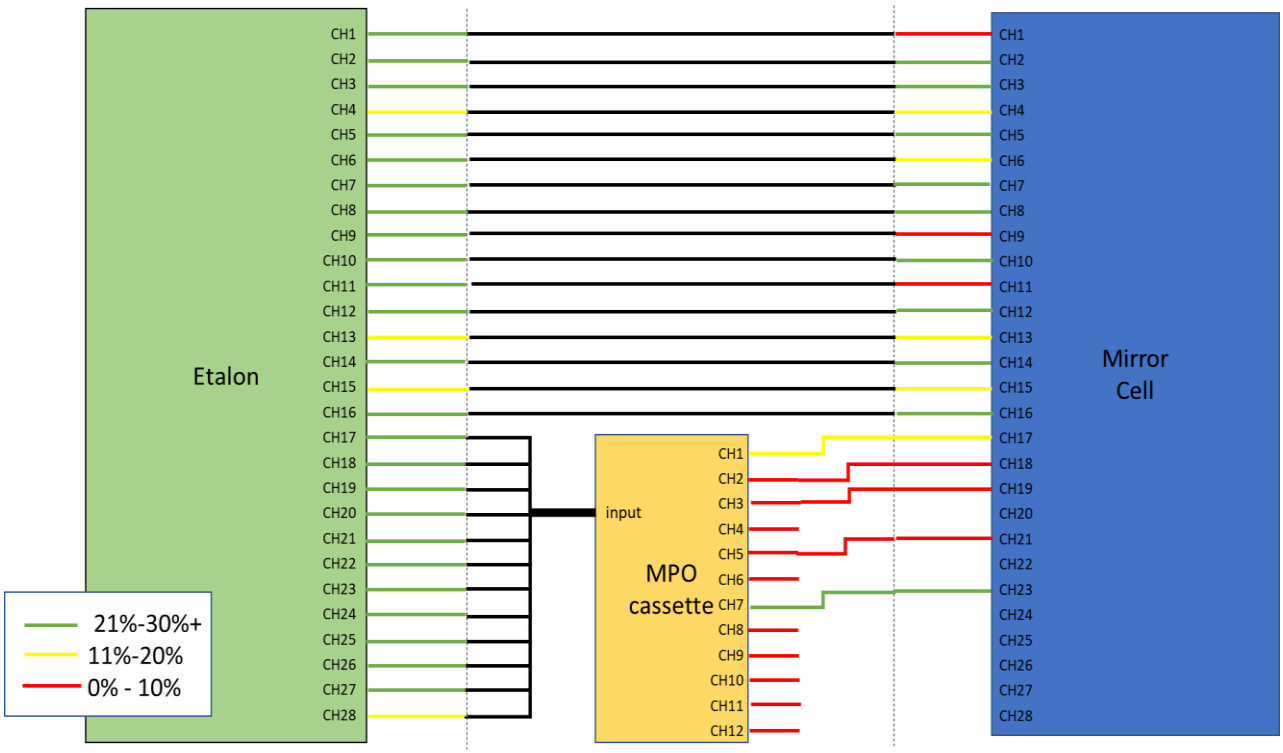

Figure 16 Channel Strength summary along the fiber route. The channel strength was analyzed at every connection point along the fiber route to troubleshoot signal loss. All 28 channels leaving the EAM had adequate signal strength. On the mirror cell only 15 channels had adequate signal strength. The MPO cassette caused signal loss in 10 channels and will need to be replaced.

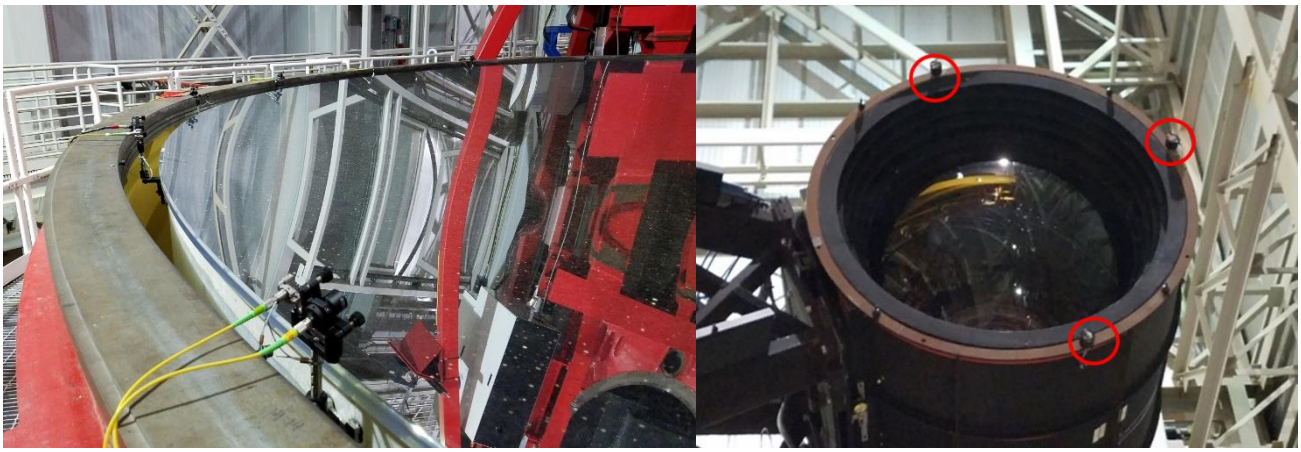

Figure 17 Collimator and retroreflector set up on LBT. There are 21 collimators on the 16 mirror cell positions. There are also two retroreflectors attached to the mirror cell to monitor the diameter of the primary mirror. Three retroreflectors are attached to the outer rim of LBC 90° apart, covering a 180° arc.

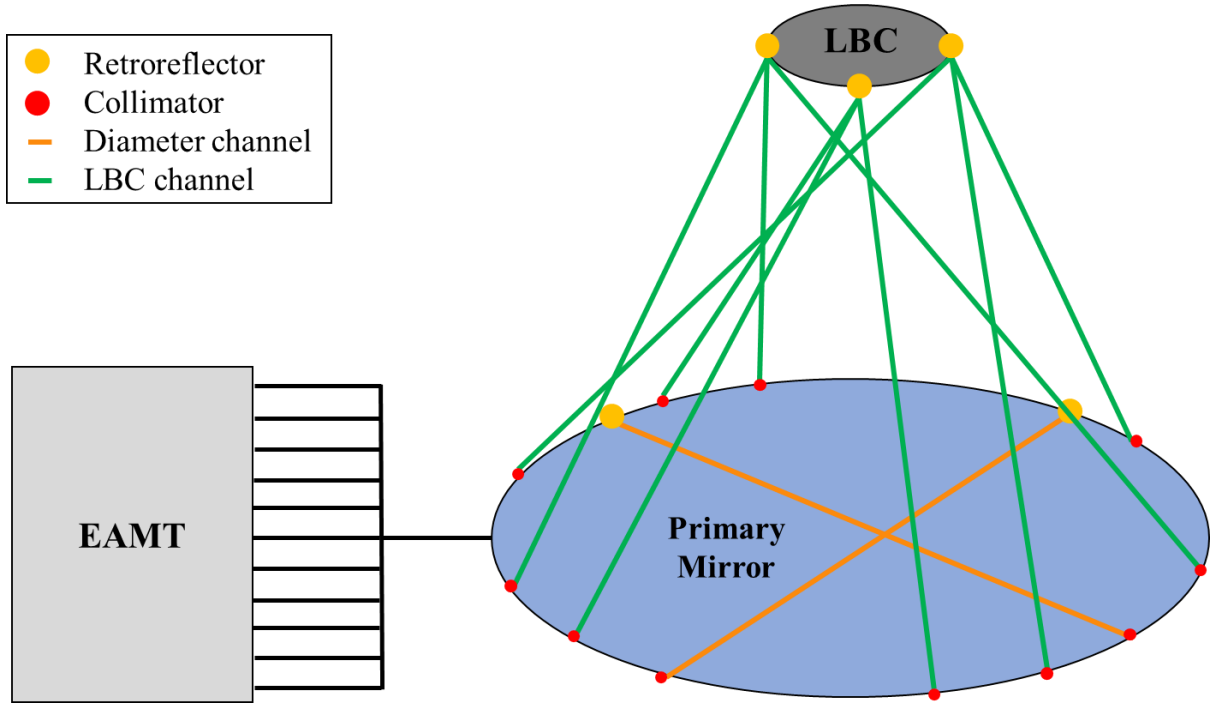

Figure 18 Collimator and retroreflector scheme on TMS. Fiber channels are routed from the EAM to the collimators around the primary mirror. The collimators are aligned to three retroreflectors on LBC to create the laser truss. Two retroreflectors on the primary mirror are used to monitor the diameter of the mirror.

An aspect of the kinematic analysis requires the positions of the retroreflectors and collimators to be defined in a reference frame. A laser tracker survey is performed to determine the location of the collimators and fiducials in space. An OmniTrac 2 laser tracker and Spatial Analysis software were used for the survey. The distance measuring accuracy is ± 25 microns and a resolution of 0.1 microns, which is sufficient for the planned use. The laser tracker comes with right angle spherical mounted retroreflectors (SMR). The SMRs are placed on whatever surface you wish to measure, either in a nest or with the sphere in contact with the surface. The the offset of the measurement from the SMR and the position you wish to measure can be set in the Spatial Analyzer software based on the size of SMR and whether it was nested or not nested. The acquired points can be extrapolated in the spatial analyzer software to create shapes, filtering out noisy points. The laser tracker survey procedure is laid out Figure 19.

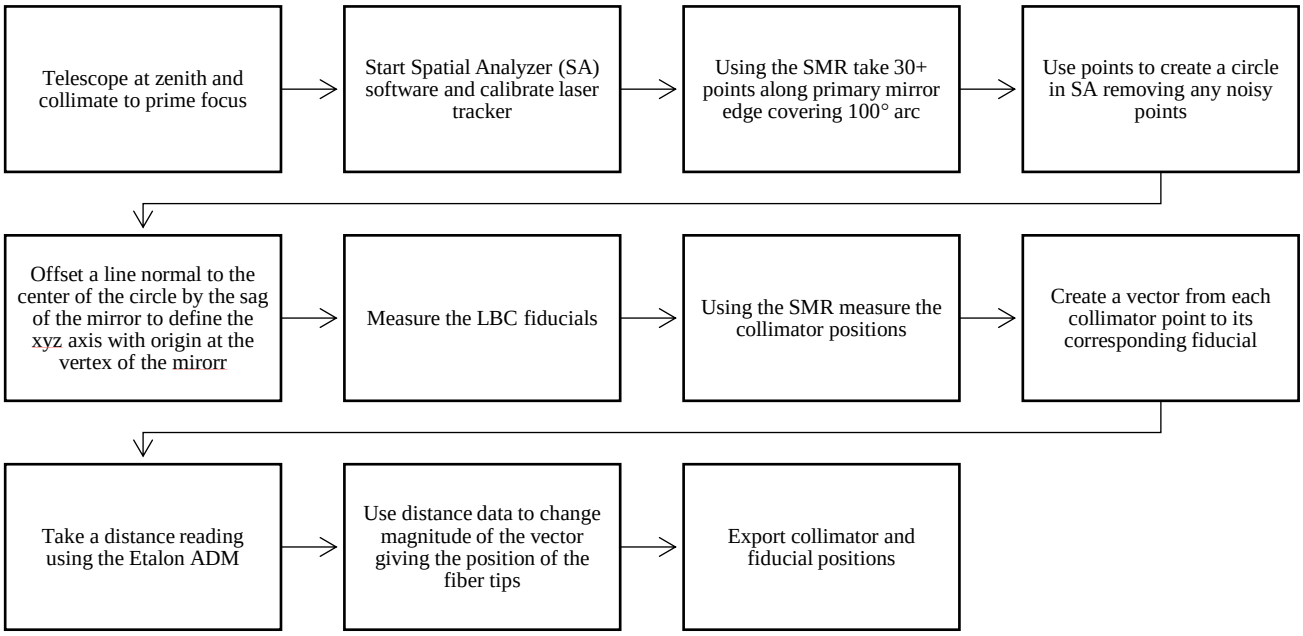

Figure 19 Laser tracker procedure used to determine the positions of all collimators and retroreflectors and to define the global reference frame. A reference frame must be defined to perform the kinematic analysis.

The survey was performed while the telescope was at zenith collimated to prime focus. First, measurement of the primary mirror is taken by obtaining a minimum of 30 points covering at least a 100° arc around the primary mirror. These points are used to render the primary mirror in Spatial Analyzer. Noisy points are removed until the RMS error is minimized. Next the position of the fiducials on LBC and LBTI c_i are measured by manual steering the laser tracker. Finally, the position of the collimators is measured. This is achieved by placing the SMR on the end of the collimator and making a measurement point ai. This allows a vector to be created between these points and the fiducials along the leg of the laser truss. EAMT measures the OPD between the measurement arm and the back reflections from the fiber tip. It is the position of the fiber tip that must be determined. The physical distance between fiber tip and the point measured by the laser tracker must be compensated. A unit vector $\vec{u}$ along the leg of the laser truss is created

$$\vec{u} = \frac{a_i - c_i}{|a_i - c_i|}$$

Then distance measurement data L_i from Etalon is taken for each leg of the laser truss. Multiplying this distance magnitude by the unit vector along the laser truss gives the position of the fiber tip b_i in the reference frame. The position of the fiber tips will from this point on be referred to simply ass the collimator position.

$$b_i = L_i\vec{u}$$

The origin of the reference frame is set as the vertex of the primary mirror. This point is not measured but calculated using the parabolic approximation of sag of the primary mirror [11].

$$sag = \frac{r^2}{2R}$$

where r is the radius of the primary mirror and R is the radius of curvature of the primary mirror. This gives an approximate sag of 460mm. These corrections can be made in the Spatial Analyzer software or post process. The results of the laser tracker survey are shown in Figure 20**Error! Reference source not found.**.

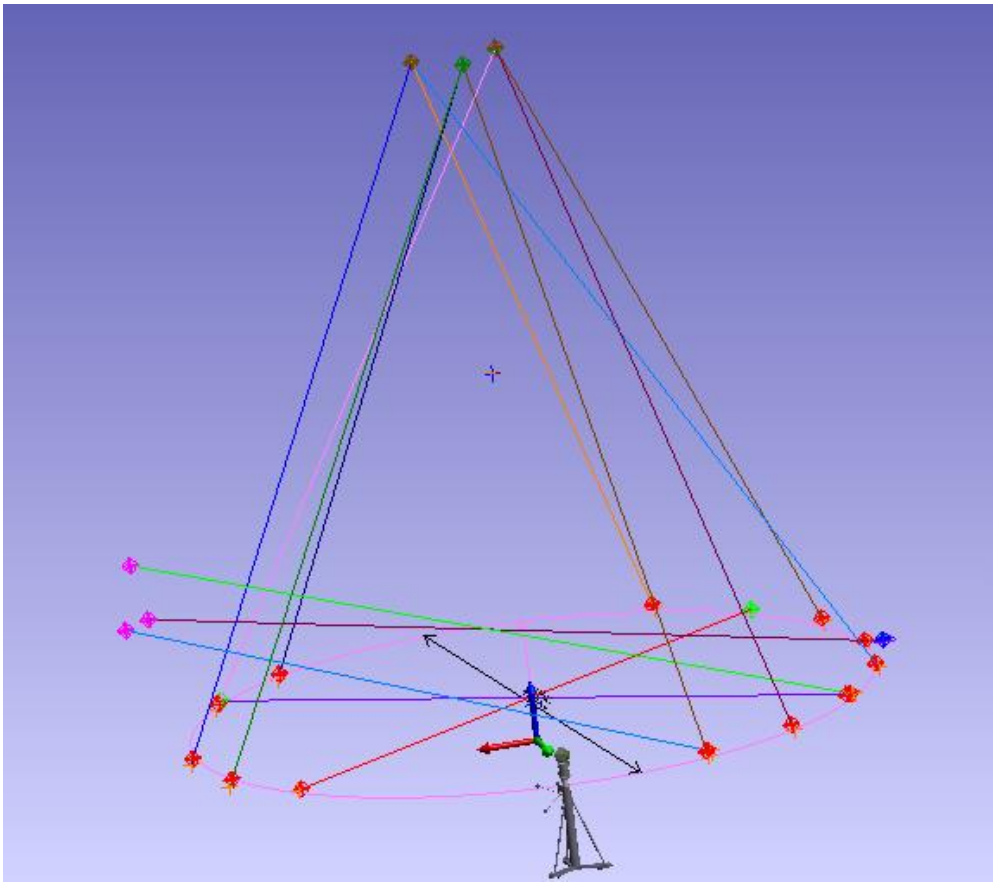

Figure 20 Laser tracker survey results. A global reference frame was created with the origin at the vertex of the primary mirror. All collimator and fiducial positions were measured. Vectors between the collimators and fiducials were created which represent the legs of the laser truss.

3. KINEMATIC ANALYSIS AND OPTICAL MODELING

With TMS functionality restored the distance data is converted into position and orientation of the primary mirror (pose). This is done using an inverse kinematic technique that will be described in Section 3.2. The pose data can then be used to maintain the optics pose and to recover the stored baseline pose.

3.1 Input data and data pipeline

Multiple applications must be used to complete the simulation process. First channel length data must be collected from the EAMT software. The EAMT collects the interferometric data from each of the channels, producing an OPD. It then corrects the OPD to a vacuum length using the Ciddor equation [9] together with temperature, pressure, and humidity data collected from its sensors. This data is then loaded into MATLAB to preform the kinematic analysis. The kinematic analysis returns data in the form of a matrix that contains x, y, and z positions and Rx, Ry, and Rz rotations for each pose of the primary mirror. A summary of the data flow is shown in Figure 21.

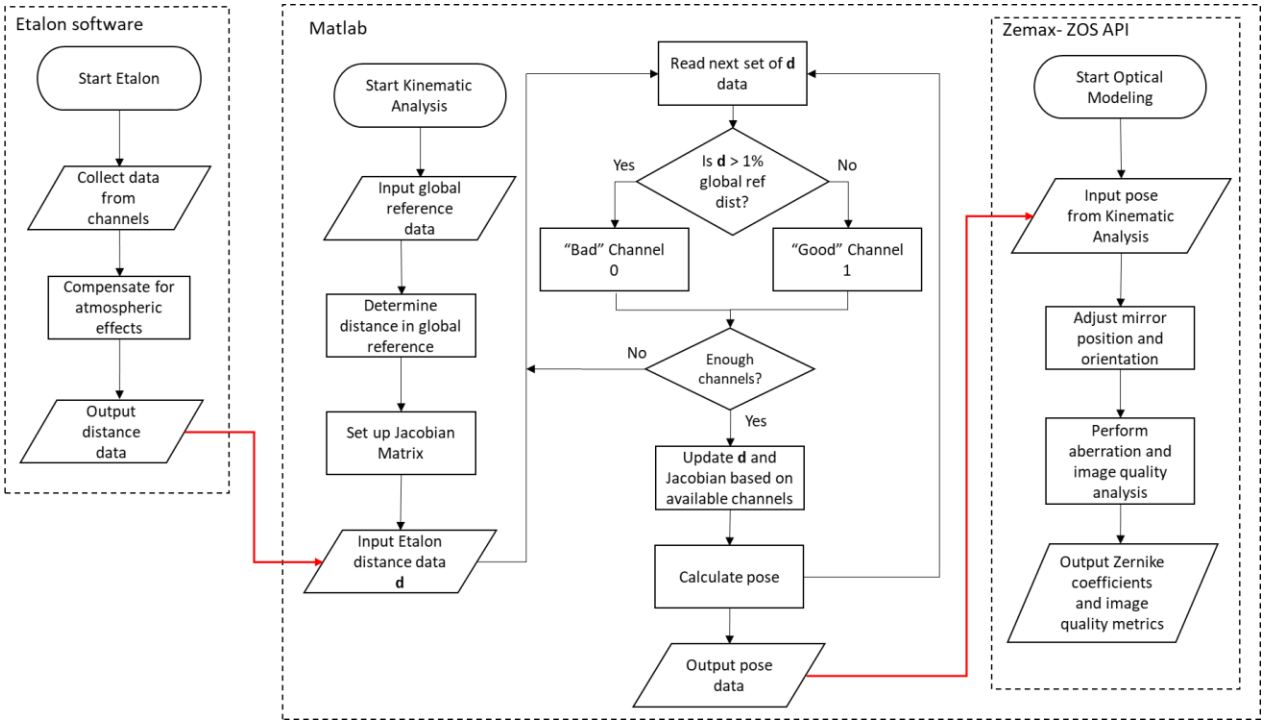

Figure 21 Data pipeline from the Etalon Absolute Multiline Technology to kinematic analysis performed in MATLAB to image quality and aberration analysis in ZOS API. Currently the process is modular, with the EAMT working independently. The red arrows indicate a transfer of data from one program to the next, which is performed manually.

Noise in the distance measurements from the Etalon can cause errors in the pose calculation. When a beam is broken the ADM still returns a distance value. This value is either very high or very small. The kinematic analysis must determine if the value given by the ADM is valid for use in the calculation. A check is performed in Matlab to make sure that the distance reading given from the Etalon is valid. Since the range of the primary mirror is known to be on the order of millimeters any large change in laser truss leg length would be impossible and must be rejected. If the leg length changes by greater than 1% of the original distance at the collimated position given by the laser tracker survey that data is invalid. This check is performed for every set of laser truss leg length data given by the Etalon. Three fiducials on LBC that comprise one end of the laser truss. A minimum of 6 laser truss legs in various configurations are needed to perform the kinematic analysis. There can be 2 channels per LBC fiducial or there can be 3,2, and 1 channels on each of the 3 LBC fiducials. Therefore

it is still possible to calculate the pose if channels are lost. If a channel is deemed "bad" it must be removed from the kinematic analysis and the Jacobian matrix must be updated before the pose can be calculated. If an insufficient number of channels are available to make a calculation the data set discarded, and the next set of data is analyzed. Therefore, it is still possible to calculate the pose if channels are lost, whether due to misalignment or damage to the fiber channel. The redundancies in the number of channels ensures that a pose calculation can be made despite noise or collimator misalignment.

3.2 Hexapod inverse kinematics using Matlab

The kinematic analysis is based on the principles of a Stewart-Gough platform in which a platform and base are connected by six legs at three points on the platform and six points on the base, creating a hexapod geometry as shown in Figure 22. A Stewart-Gough platform is a mechanical system which uses actuators to drive changes in the length of the legs inducing a change the position of the platform. For the TMS, the legs of the platform are the channels of the EAMT constituting the laser truss between the primary mirror and the LBC. In a traditional Stewart-Gough platform forward kinematics are used to map desired changes in position and orientation of the platform to changes in leg length. In the case of TMS on LBT, the leg length is known, and the position and orientation of the primary mirror must be determined. This is accomplished using an inverse kinematic technique, which produces a Jacobian sensitivity matrix for relating leg-length changes to modal pose changes, then uses the Moore-Penrose pseudoinverse of this matrix to calculate modal pose changes from a vector of leg-length changes [12].

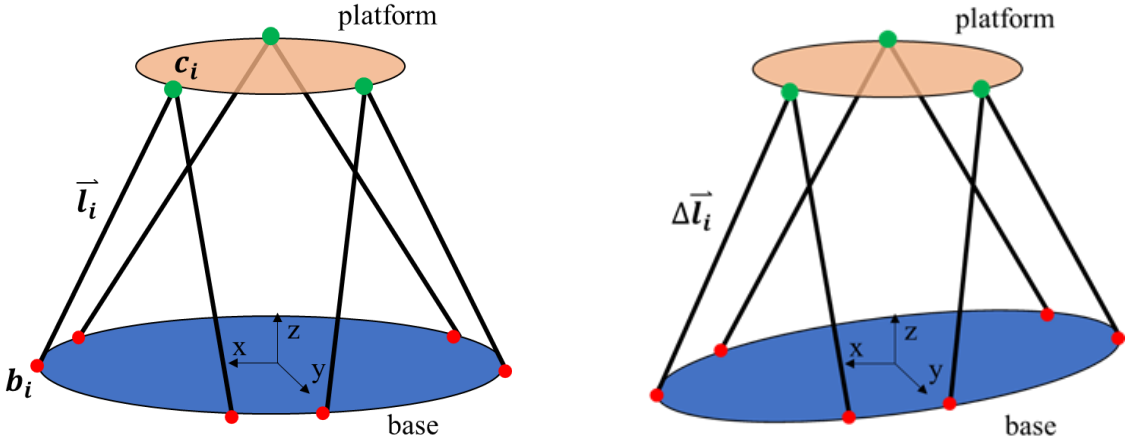

Figure 22 The Stewart-Gough platform in its initial position consists of a platform held parallel to a base supported by legs of length l (left). Changes in leg length Δl are made to move the platform to a desired position and orientation relative to the stationary base (right).

The Jacobian matrix is the foundation of the kinematic analysis technique is defined first. The Jacobian matrix defines sensitivity of position and orientation changes in the platform (pose) relative to the base to changes in truss leg length. When the Jacobian is multiplied by the changes in pose and orientation the change length of the legs of the platform is defined by

$$^{l}SC_x\hat{x} = \Delta l$$

where ${}^{l}SC_x$ is the Jacobian matrix, $\hat{x}$ is the pose matrix, and Δl is the changes in leg length corresponding to the desired change in pose. This is a simple linear algebra equation that is the basis for the kinematic analysis of a Stewart-Gough platform.

The Jacobian is formed using the global reference data obtained during the laser tracker survey. First the laser truss legs must be established.

$$l_i = c_i - b_i$$

The legs of the laser truss are defined as vector l_i between fiducial points c_i and the collimator points b_i as determined by the laser tracker survey. To simplify the calculation the unit vector $\widehat{e_i}$ of l_i is used.

$$\widehat{e_i} = \frac{l_i}{|l_i|}$$

where $\widehat{e_i}$ is the unit vector of the i[th] leg of the truss.

The Jacobian matrix ${}^{l}SC_x$ is created by cross multiplying the position of the retroreflectors c_i with the unit vector $\widehat{e_i}$ for the i[th] leg of the truss and then taking the transpose. This defines the sensitivities to rotation of the primary mirror around its x, y, and z axis with origin at the vertex of the primary mirror. The sensitivities to tranlation are the transpose of the unit vector of the ith leg of the truss and make up the last column of the matrix.

$${}^{l}SC_x = \begin{vmatrix} (c_1 \times \widehat{e_1})^T & \widehat{e_1}^T \\ \vdots & \vdots \\ (c_n \times \widehat{e_n})^T & \widehat{e_n}^T \end{vmatrix}$$

The Jacobian is a nx6 matrix that defines the system sensitivity to the six degrees of freedom in rotation and translation.

When using forward kinematics, the Jacobian is multiplied by the desired position and orientation to determine the changes in leg length needed to achieve the desired pose.

$$\left(\begin{pmatrix} {}^{1}SC_1 & \cdots & {}^{1}SC_m \\ \vdots & \ddots & \vdots \\ {}^{n}SC_1 & \cdots & {}^{n}SC_m \end{pmatrix} \right) \begin{pmatrix} \theta_x \\ \theta_y \\ \theta_z \\ x \\ y \\ z \end{pmatrix} = \begin{pmatrix} \Delta l_1 \\ \vdots \\ \Delta l_n \end{pmatrix}$$

To map changes in laser truss leg length to changes in position and orientation the inverse of the Jacobian matrix ${}^{x}SC_l$ must be used. This is the inverse kinematic technique.

$${}^{x}SC_l = \left({}^{l}SC_x \right)^{-1}$$

The inverse Jacobian can then be used to determine the pose for any given data set of laser truss leg lengths using a simple matrix multiplication.

$$\hat{x} = \left({}^{l}SC_x \right)^{-1} \widehat{\Delta l}$$

where $\hat{x}$ is the pose matrix defining the position and orientation of the primary mirror and $\widehat{\Delta l}$ is the change laser truss leg length as reported by the EAMT. Note that the over-determined system described above in general produce a matrix that is non-invertible, but in such cases the pseudoinverse provides the optimum solution.

It is important to note that the technique described above differs from that used in reference 3, in which case the EAMT system software was used to give point deflections of each retroreflector. The new technique has several advantages over what has been done previously, allowing dynamic channel deletion and the use of telescope temperature telemetry to perform airpath compensation of the distance data. This also allows for easier integration of TMS into the telescope control system to actively align the primary mirror.

3.3 Optical Modeling Using TMS Data

Now that the pose of the primary mirror has been determined using kinematic analysis, that data can be integrated into an optical model. This allows for a wide variety of simulation and analysis to be performed using measured telescope position and orientation. An optical model of the LBT in prime focus mode, including the optical elements of the LBC are modeled (Figure 23). The goal of optical modeling is to determine how misalignment of the telescope effects the image. The optical elements are assumed to maintain their shape. In reality, the optics will endure bending, mechanical strain, and thermal expansion. Those considerations are outside the current scope of this project, but may be considered in future iterations the metrology methodology using mechanical simulation analysis.

The pose data from TMS in MATLAB is input into the optical model using the Zemax OpticStudio Application Interface (ZOS-API). Pose is given as lateral xyz displacement and Rx Ry Rz rotational displacement. The position of the primary mirror is iteratively controlled for each set of TMS pose data. The LBC optical elements remain fixed. At each pose of the primary mirror system performance can be analyzed. The effect of system misalignment propagates through the system and can be examined at the image plane. When using TMS data from on sky observation the image simulation using the optical model can be compared to LBC data and images.

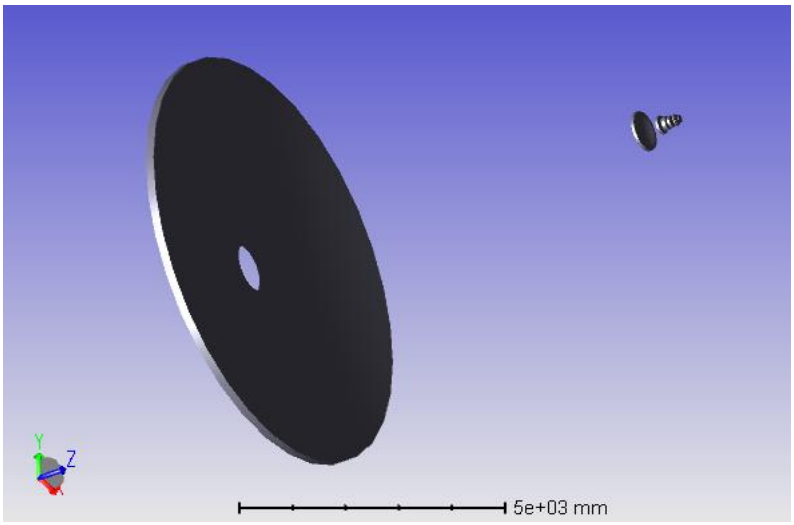

Figure 23 Optical model using Zemax OpticStudio. Modeled is the primary mirror and all of the optical elements of LBC. TMS pose data can be input into the model to move the primary mirror. Aberration and image quality analysis can be performed for each set of pose data.

4. SIMULATION ANALYSIS OF TMS

4.1 Test using known movement

To validate the TMS, the telescope control system (TCS) was used to induce known primary mirror movement. The telescope motions were then compared to the pose data from the TMS.

The test was performed in stable environmental conditions, at zenith under a closed dome. Keeping the telescope at zenith, ensures that there are no varying deflections in mirror position due to gravitational effects. Performing the test under a close dome minimizes the amount of errors due to environmental fluctuations such as rapid changes in ambient temperature humidity, and pressure. Each of the six degrees of freedom of movement of the primary mirror were individually tested. The primary mirror was moved incrementally over the full range of motion or until the beams of the laser truss were broken which is over the normal telescope operation mode. The results of the induced rotational and lateral motion are shown in Figure 24.

The calculated pose showed a maximum deviation from TCS controls for the given set of data of 1.7μm for lateral motion and 0.1 arcsec for rotational motion. These are within the expected range or deviation, and account for a very small percentage of the commanded motions. These deviations cannot be attributed to error in pose calculation alone. There are other sources of error that contribute to deviations from TCS controls. Data is only compared to TCS controls at periods when the primary mirror is stationary. The data was taken with relatively short periods of rest at each step in the motion, which could cause oscillation in the primary mirror position as it stops and starts motion. It is also possible that there is hysteresis in the mechanisms that control primary mirror movement. If TCS is not accurately driving the primary mirror position this will compound the error between TCS control inputs and TMS pose data. Fortunately, the error is also relatively small compared to the requirements of telescope alignment. The system's ability to contribute to telescope alignment has been validated [8]. It is reasonable to expect that the small percent of error in pose calculation will not greatly impact system performance.

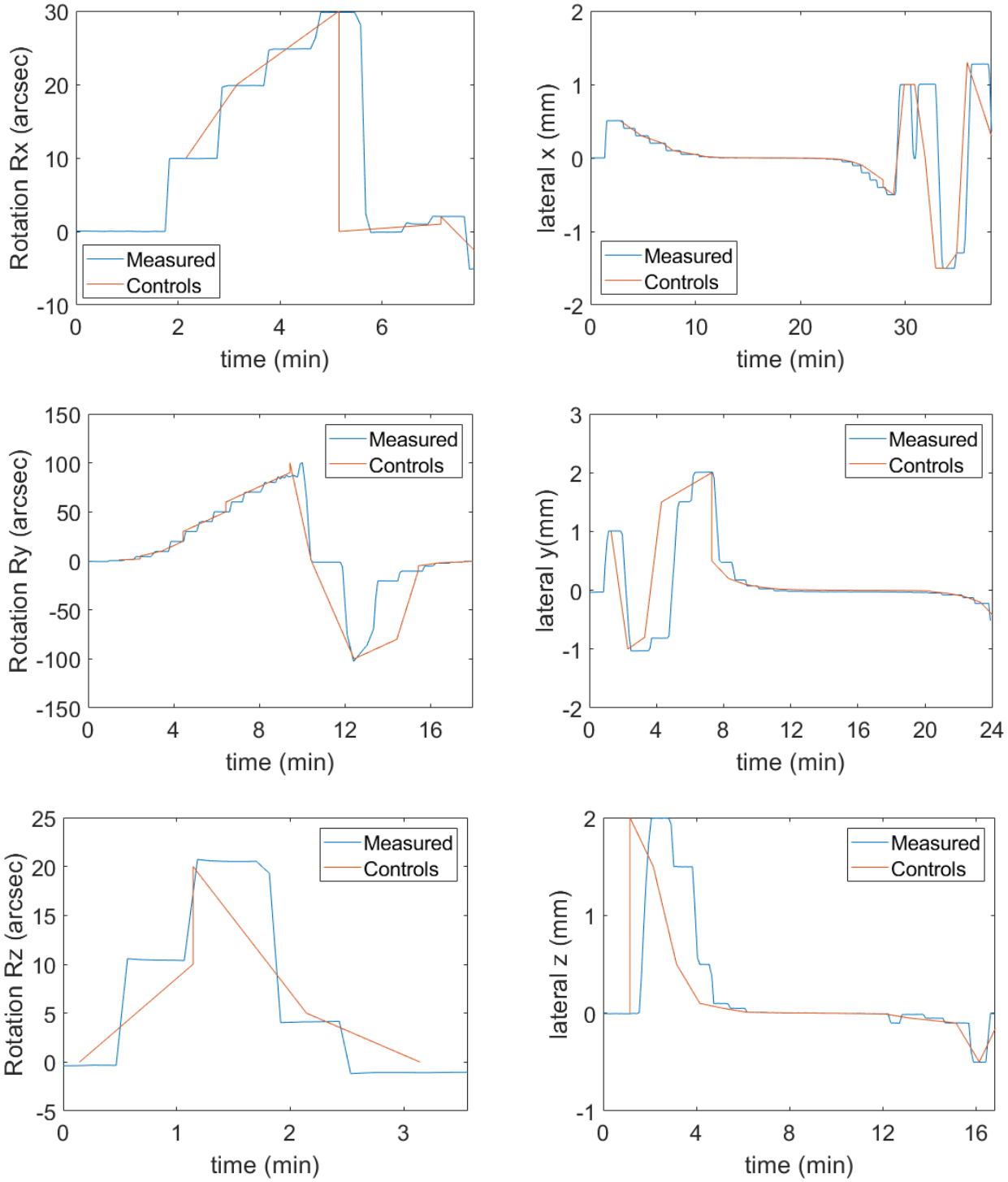

Figure 24 TMS data for Rx, Ry, and Rz rotational (left) and x, y, and z lateral motion (right). In all plots the red line represents the induced motion of the primary mirror and the blue line corresponds to the measured change in position and orientation. For all controlled steps in motion TMS determined the corresponding pose, although there is some delay due to different sampling times between TCS and TMS.

5. IMAGE ANALYSIS USING TMS OPTICAL MODEL

Once the validity of the pose of the TMS data was verified it could then be used to perform aberration and image analysis using an optical model. This allows for a wide variety of simulation and analysis to be performed using measured telescope position and orientation. An optical model of the LBT in prime focus mode, including the optical elements of the LBC are modeled. The goal of optical modeling is to determine how misalignment of the telescope affects the star image. The optical elements are assumed to maintain their shape, though in reality, the optics will endure bending, mechanical strain, and thermal expansion. Such considerations are outside the current scope of this project but are being be considered in ongoing development of the metrology methodology using mechanical simulation analysis.

The pose data from TMS is input into the optical model. Pose is given as lateral x, y, and z displacement and Rx, Ry, and Rz rotational displacement. At each pose of the primary mirror system performance is analyzed. The effect of system misalignment propagates through the system and is examined at the image plane. When using TMS data from on-sky observation, the image simulation using the optical model can provide the expected image quality for all fields and guide the pointing and collimation procedure.

5.1 Aberration analysis

Performing aberration analysis can help determine what aberrations are caused purely by optical misalignment, making it possible to disentangle misalignment aberrations from aberrations caused by other factors [13]. This information can be used to determine what kind of corrections to primary mirror position need to be made to improve image quality. Using a TMS data set taken over induced Rx motion the Zernike coefficients for first order coma are shown in Figure 25. Coma was observed for both the on-axis and off-axis field. Z7 is oriented parallel to the increase in field angle and the field dependence is seen. Z7 shifts in magnitude at an off-axis field position. Z8 is oriented perpendicular to the field and therefore it does not have field dependence in that direction.

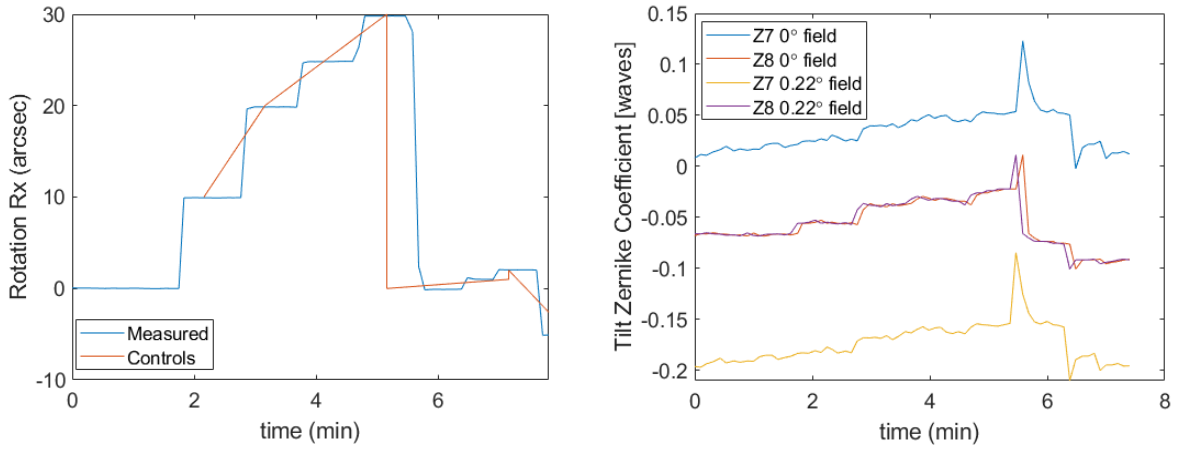

Figure 25 Aberration analysis for induced Rx motion. The first order coma Zernike terms are shown for on-axis and off-axis fields (right) for the Rx motion of the primary mirror (left). The off axis field is in the y direction. The field dependence of Z7 is shown. Z8 has no field dependence.

5.2 Image quality analysis

Simulated image quality using the TMS pose data can help determine what affect misalignments have on the image obtained by LBC. Misalignment of the primary mirror can cause aberrations that propagate to the image plan. This can be used to determine corrections to primary mirror position needed to improve image quality. Images obtained using the modeling can also be compared to images obtained by LBC using the pose data from the exposure.

When an optical system is decentered or tilted it becomes non-rotationally symmetric. A viable tool when analyzing a non-rotationally symmetric optical system is a spot diagram. In a more practical sense, when viewing star images, the spot size and shape produced in the optical model can indicate misalignment patterns like those observed with FPIA. The change in RMS spot size due to lateral x decenter is shown in Figure 26 and Figure 27. Spot size analysis only shows changes in magnitude, not sign. Using TMS data the sign ambiguity of the change in spot size can be resolved.

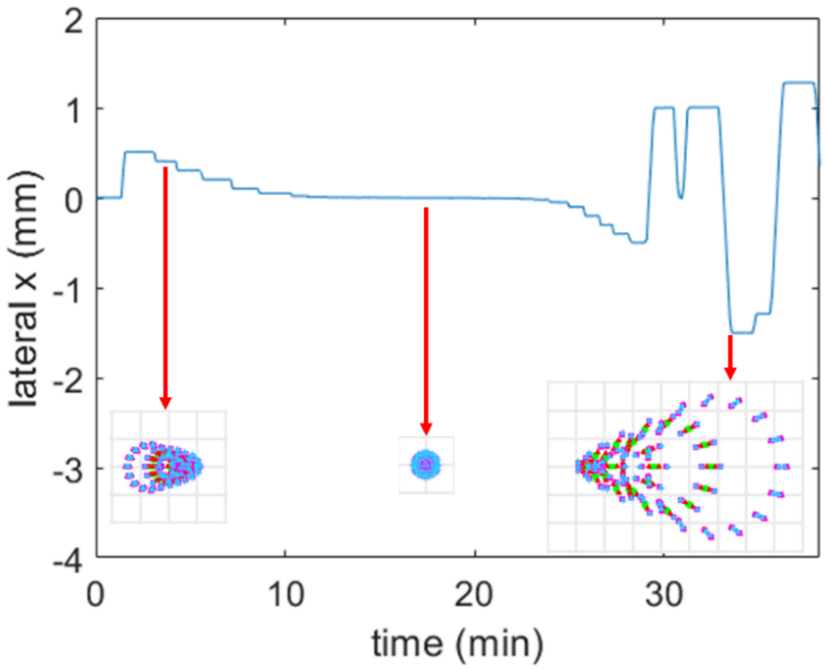

Figure 26 As the lateral x motion of the primary mirror is induce the spot size will undergo changes in shape. The spot diagrams shown at the bottom of the figure are to scale. As displacement from the center increase the size of the spot also increases.

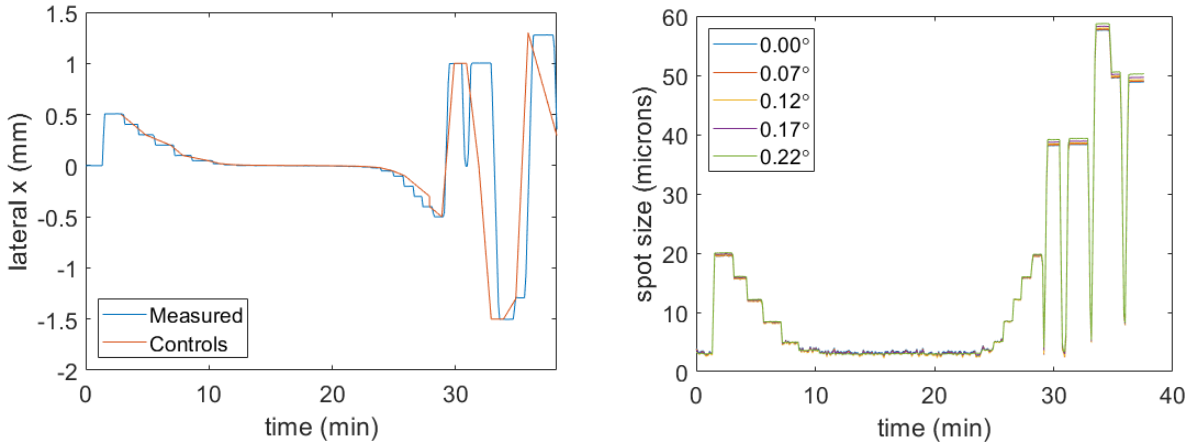

Figure 27 The effect of lateral x decenter (left) on the image RMS spot size (right). Using TMS pose data the spot size is determined across several fields and is found to correlate well to the induced lateral motion.

6. CONCLUSION AND FUTURE WORK

Functionality of TMS was achieved at prime focus in monocular mode. The position and orientation of the primary mirror and LBC was successfully determined using an inverse kinematic analysis of noise-filtered EAMT distance data with a lateral deviation of 1.7 µm and rotational deviation of 0.1 arcseconds. TMS pose data was integrated into an optical model. The optical model was used to iteratively perform image quality and aberration analysis.

The next step in the prototyping process is preparing TMS for binocular use at prime focus. Fortunately, the process for deploying TMS on the SX side of the telescope is identical to the process for the DX side. The same kinematic analysis can be used with modifications to the Jacobian based on the difference between the collimator and retroreflector positions on the SX and DX sides.

The proposed metrology technique has been verified by using controlled movements of the primary mirror. The system will be used to passively monitor primary mirror position during on-sky observation with LBC and the results correlated to image quality data from FPIA. Once system performance is verified using passive monitoring TMS will be integrated into the telescope control system to actively control the telescope alignment. The final two phases of the prototyping process require implementation of TMS for direct and bent Gregorian focal modes.

7. REFERENCES

[1] D. S. Ashby, C. Biddick and J. M. Hill, "Active optics control development at the LBT," in *SPI Astronomical Telescopes + Instrumentation*, Montreal, Quebec, Canada, 2014.

[2] J. M. Hill, "The Large Binocular Telescope," *Applied Optics*, vol. 49, no. 16, 2010.

[3] R. Speziali and e. al., "The Large Binocular Camera: description and performances of the first binocular imager," in *Proceedings of SPIE*, 2008.

[4] D. Terret, *Active Optics and Pointing on LBT*, LBT internal document, 2006.

[5] J. Hill, R. Ragazzoni, A. Baruffolo, C. Biddick, O. Kuhn and e. al., "Prime focus active optics with the Large Binocular Telescope," in *Proceedings of SPIE*, Marseille, 2008.

[6] R. Wilson, Reflecting Telscope Optics II, Springer, 1999.

[7] A. Rakich, L. Dettmann, S. Leveque and S. Guisard, "A 3D metrology system for the GMT," *Proceedings of SPIE*, vol. 9906, no. SPIE Astronomical Telescopes + Instrumentation, 2016.

[8] A. Rakich, P. Schurter, R. Conan, J. Hill, M. Gardiner, M. Bec and O. Kuhn, "Prototyping the GMT telescope metrology system on LBT," *SPIE*, 2018.

[9] J. Dale, B. Hughes, A. J. Lancaster, A. J. Lewis, A. J. Reichold and M. S. Warden, "Multi-channel absolute distance measurement system with sub ppm-accuracy and 20 m range using frequency scanning interferometry and gas absorption cells," *Optics Express*, vol. Vol. 22, no. No. 20, 2014 .

[10] P. E. Ciddor, "Refractive index of air: new equations for the visible and near infrared," *Applied Optics*, vol. 35, no. 9, pp. 1566-1573, 1996.

[11] J. E. Greivenkamp, Field Guide to Geometrical Optics, Bellingham: SPIE, 2004.

[12] J. Nissen, "GMT Laser Metrology Truss," GMT Internal Document, 2019.

[13] A. Rakich, J. M. Hill, C. Biddick, D. Miller and T. Leibold, "Use of field aberrations in the alignment of the Large Binocular Telescope optics," in *PROCEEDINGS OF SPIE Astronomical Telescopes + Instrumentation*, Marseille, France, 2008.